

Characteristics of solar-like oscillations in red giants observed in the CoRoT^{*} exoplanet field

S. Hekker^{1,2,3}, T. Kallinger⁴, F. Baudin⁵, J. De Ridder², C. Barban⁶, F. Carrier², A.P. Hatzes⁷, W.W. Weiss⁴, and A. Baglin⁶

¹ University of Birmingham, School of Physics and Astronomy, Edgbaston, Birmingham B15 2TT, United Kingdom
e-mail: saskia@bison.ph.bham.ac.uk

² Instituut voor Sterrenkunde, K.U. Leuven, Celestijnenlaan 200D, 3001 Leuven, Belgium

³ Royal Observatory of Belgium, Ringlaan 3, 1180 Brussels, Belgium

⁴ Institute for Astronomy, University of Vienna, Türkenschanzstrasse 17, A-1180 Vienna

⁵ Institute d' Astrophysique Spatiale, UMR 8617, Université Paris XI, Bâtiment 121, 91405 Orsay Cedex, France

⁶ LESIA, UMR8109, Université Pierre et Marie Curie, Université Denis Diderot, Observatoire de Paris, 92195 Meudon Cedex, France

⁷ Thüringer Landessternwarte, D-07778 Tautenburg, Germany

Received ; accepted

ABSTRACT

Context. Observations during the first long run (~ 150 days) in the exo-planet field of CoRoT increase the number of G-K giant stars for which solar-like oscillations are observed by a factor of 100. This opens the possibility to study the characteristics of their oscillations in a statistical sense.

Aims. We aim to understand the statistical distribution of the frequencies of maximum oscillation power (ν_{max}) in red giants and to search for a possible correlation between ν_{max} and the large separation ($\Delta\nu$).

Methods. Red giants with detectable solar-like oscillations are identified using both semi-automatic and manual procedures. For these stars, we determine ν_{max} as the centre of a Gaussian fit to the oscillation power excess. For the determination of $\Delta\nu$, we use the autocorrelation of the Fourier spectra, the comb response function and the power spectrum of the power spectrum.

Results. The resulting ν_{max} distribution shows a pronounced peak between 20 - 40 μ Hz. For about half of the stars we obtain $\Delta\nu$ with at least two methods. The correlation between ν_{max} and $\Delta\nu$ follows the same scaling relation as inferred for solar-like stars.

Conclusions. The shape of the ν_{max} distribution can partly be explained by granulation at low frequencies and by white noise at high frequencies, but the population density of the observed stars turns out to be also an important factor. From the fact that the correlation between $\Delta\nu$ and ν_{max} for red giants follows the same scaling relation as obtained for sun-like stars, we conclude that the sound travel time over the pressure scale height of the atmosphere scales with the sound travel time through the whole star irrespective of evolution. The fraction of stars for which we determine $\Delta\nu$ does not correlate with ν_{max} in the investigated frequency range, which confirms theoretical predictions.

Key words. stars: red giants – stars: oscillations – methods: observational – techniques: photometric

1. Introduction

Before the CoRoT era, the presence of solar-like oscillations was firmly established for a few red (G-K) giant stars only. We refer to De Ridder et al. (2009) for an overview of these results. With this low number of firm detections, different authors reached different conclusions in terms of the presence of only radial modes with short lifetimes or radial and non-radial oscillation modes with much longer lifetimes.

Observations with CoRoT increased the number of giants with a clear detection of solar-like oscillations by almost a factor of 100. Using these observations, De Ridder et al. (2009) recently presented the discovery of non-radial oscillations modes with long lifetimes (≥ 50 days). This result is important for red giant seismology, not only because the frequencies of modes

with long lifetimes can be more precisely determined, but also because non-radial modes contain more information about the internal structure of giants than radial modes only.

Subsequently, Kallinger et al. (2009) derived for 31 giants in the sample of De Ridder et al. (2009), the frequency of maximum power and the large separation, and used these values to estimate the mass and the radius.

In the present paper, we exploit the fact that we now have, for the first time, a large sample of red giants with established solar-like oscillations, which opens up the possibility to analyse the characteristics of the power spectrum in a statistical way. In particular, we investigate the distribution of the frequency of maximum oscillation power ν_{max} , and the large frequency separations $\Delta\nu$, i.e. the frequency difference between modes with the same degree and consecutive orders. These parameters change with stellar age, and their histogram can therefore provide insight into the population of observed giants.

* The CoRoT space mission which was developed and is operated by the French space agency CNES, with participation of ESA's RSSD and Science Programmes, Austria, Belgium, Brazil, Germany, and Spain. Light curves can be retrieved from the CoRoT archive: <http://idoc-corot.ias.u-psud.fr>.

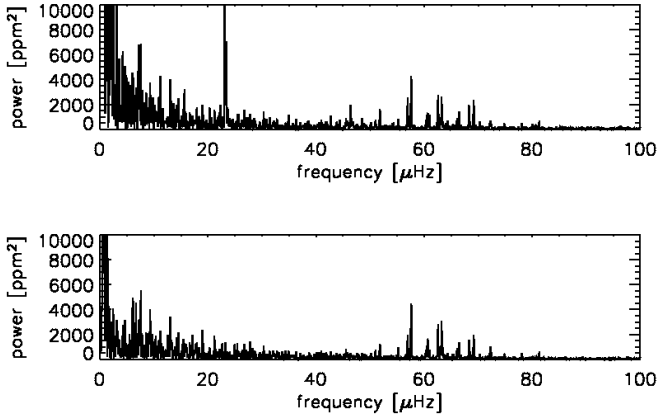


Fig. 1. Uncorrected (top) and corrected (bottom) power spectrum of the star with corot-id 100697490. The peak at about $23\ \mu\text{Hz}$ is twice the daily frequency.

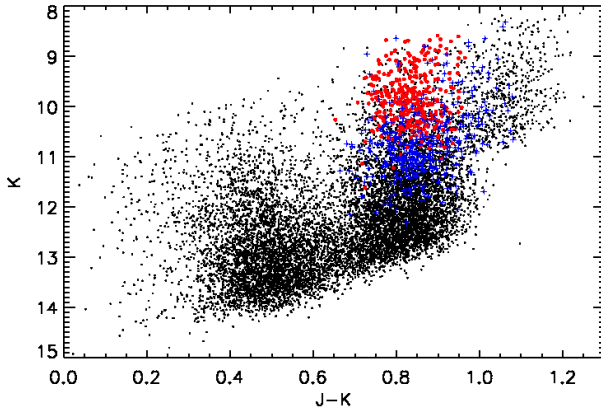


Fig. 2. Colour-magnitude diagram of the observed field stars using the J and K photometric passbands (Deleuil et al. 2006). The red dots represent the semi-automatic selected red giants and the blue crosses the ones selected by eye only. The black dots represent all other targets in the field. Note that these photometric data have not been dereddened.

2. Data

The CoRoT data used in this work are the reduced (N2) monochromatic light curves (Auvergne et al. 2009) provided by the CoRoT data centre of the first long run (LRc01) of about 150 days from May to October 2007, when the satellite was pointed towards the galactic centre ($(\alpha, \delta) = (290.89^\circ, 0.46^\circ)$). For information on the CoRoT data reduction, we refer to Baglin & Chaintreuil (2006). The data used for the present investigation are obtained in the so-called exofield. The light curves consist of approximately 330 000 points with a typical time step of 32 s. Although the light curves of some of the targets of interest contain fewer data points, with a cadence of 512 s. In all data sets, we removed all points that were flagged as unreliable.

Many of the light curves show signs of instrumental effects. A proper treatment of these effects would require an in-depth knowledge of the instrument and is currently under investigation by the CoRoT data centre. For the purpose of this paper it suffices to mitigate the instrumental effects as follows. First, we

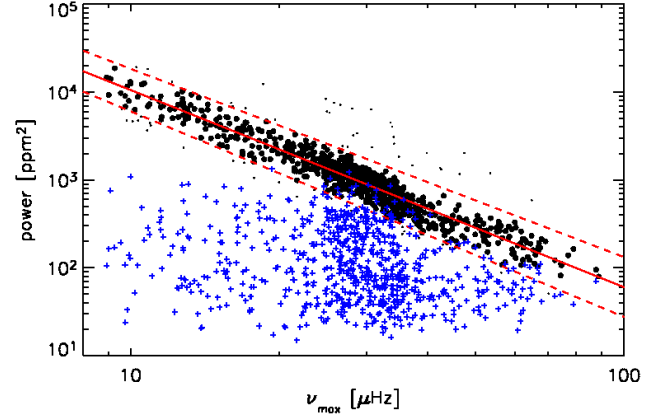


Fig. 3. The height of the oscillation power excess (D in Eq. 1) is shown as a function of ν_{\max} with black dots (outliers are indicated with smaller dots). The solid red line represents the linear fit in log space $D = 6.3 - 2.2\nu_{\max}$, with the 3σ interval indicated with red dashed lines. The blue crosses represent white noise (E in Eq. 1, further discussed in Section 4.1).

eliminated possible trends by fitting and subtracting a second-order polynomial. Secondly, the occasional jumps due to high-energy particles were first detected by comparing flux-levels in consecutive time intervals at least 10 times larger than the expected oscillation periods, and were then removed by fitting and subtracting a polynomial background on each side of the jump. Finally, outliers were removed using a 4-sigma clipping around the mean flux value. Comparing the power spectra of the corrected time series with power spectra of the uncorrected time series, revealed that the instrumental effects are not dominant, see Fig. 1 for an example. To see the effect at low frequencies, we looked at the power spectra of B stars, for which the noise at low frequencies should be dominated by instrumental noise, as there is no surface granulation for these stars. Assuming that the instrumental noise for B stars is roughly the same as for giants, we could conclude that the low-frequency noise in the red giant power spectra is not dominated by instrumental noise, with only a few exceptions in cases with a large number of jumps.

3. Identification of oscillations in red giants

Visual and near-IR photometry are available for all stars observed in the exo-field during run LRc01 (Deleuil et al. 2006). These colours are affected by reddening, but as shown by Bessell & Brett (1988) near-IR colours are least affected, and provide a first estimate of the spectral type. A J-K versus K colour-magnitude diagram is shown in Fig. 2.

Red giants with solar-like oscillations cannot (yet) be classified with the automated supervised classification algorithm developed for CoRoT (Debosscher et al. 2007). This is mainly due to the low amplitudes of these oscillations and the low number of detections prior to CoRoT observations. These low numbers hamper a reliable class definition, which is needed by the classification algorithm used by Debosscher et al. (2007).

We used the same semi-automatic procedure as described by De Ridder et al. (2009) to select red-giant stars for which we can detect solar-like oscillations. In addition, for reasons explained below, we also inspected the Fourier spectra by eye to check for oscillation features in stars not selected with the semi-automatic procedures. In the selection by eye we inspected the power spec-

trum between 0 and 120 μHz for broad power excess (in case of modes with short lifetimes) or a cluster of several individual frequency peaks at intervals of a few μHz (modes with long lifetimes). At $\sim 163 \mu\text{Hz}$ a strong frequency peak due to the orbital period of CoRoT is present which has sidelobes at intervals of $11.57 \mu\text{Hz}$ down to about $120 \mu\text{Hz}$. These features in the power spectrum limit the frequency range for which we search for oscillation signatures.

To validate our selection we fitted a model to the smoothed power spectrum consisting of a power law and a Gaussian representing the oscillation power excess respectively, see Eq. 1, with ν the frequency, A the amplitude of the background, B the characteristic timescale, C the slope of the power law, D the height of the oscillation power excess, ν_{\max} the frequency of maximum oscillation power, σ the width of the oscillation excess and E the white noise. The smoothing is performed using a moving average with a varying width of 4 times the expected large separation at each frequency (Kjeldsen et al. 2008). See Section 4 for the correlation between $\Delta\nu$ and ν_{\max} . We take frequency changes in the oscillation spectrum into account in the smoothing to pursue a homogeneous analyses for all stars in the sample.

$$P(\nu) = \frac{A}{(1 + (B \cdot \nu)^C)} + D \cdot e^{\frac{(\nu_{\max} - \nu)^2}{2\sigma^2}} + E, \quad (1)$$

This fitting procedure is a simplification of the background fitting used by Aigrain et al. (2004), which is sufficient as we only use it to validate the presence of the oscillations and pinpoint their frequency of maximum oscillation power (Section 4.1).

For the validation of our candidates, we first removed stars with non-converging or spurious fits from the sample. Then we looked into the fitted height of the power excess (D in Eq. 1). Chaplin et al. (2009) recently presented a scaling relation for mode lifetimes and they find that the maximum mode height of the oscillations (H) depends predominantly on the surface gravity of stars (g), i.e., $H \sim g^{-2}$. Furthermore, it is known that $\nu_{\max} \sim \nu_{ac} \sim g T_{\text{eff}}^{-1/2}$, with ν_{ac} the acoustic cut off frequency (Brown et al. 1991; Kjeldsen & Bedding 1995). Combining these 2 relations, in which we approximate the effective temperature (T_{eff}) to be constant, we expect that $H \sim \nu_{\max}^{-2}$ and thus also that the height of the Gaussian fit to the oscillations power excess decreases with increasing ν_{\max} . In Fig. 3, we indeed see the expected trend and the best fit provides us with an exponent of -2.2 instead of -2, which is predicted by the scaling relation. This may be due to the fact that the scaling relation for H is based on narrow band photometry, while we use the height of the power excess in broadband photometry.

As we expect that the scaling relations should be valid for all stars at hand, we exclude stars with fit parameters which fall outside the 3σ interval around the correlation between the fitted height of the oscillation excess and the frequency of maximum oscillation power. This left us with 778 oscillating red giant candidates, which are indicated in Fig. 2 and in the online Table 1.

4. Characteristics of solar-like oscillation in red giants

4.1. Frequency of maximum oscillation power

The frequency of maximum oscillation power, defined as the centre of the Gaussian fitted to the oscillation power excess, is the first parameter of interest we investigate here. The ν_{\max} distribution is plotted in Fig. 4. This distribution shows a clear maximum between 20-40 μHz . Before interpreting this distribution,

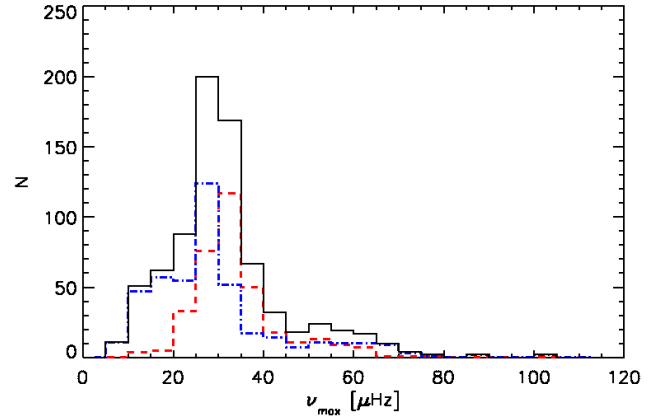


Fig. 4. The histogram of the frequencies at maximum oscillation power for all oscillating red-giant candidates is shown in black. The red dashed and blue dash-dot histograms show the ν_{\max} distribution for oscillating red giants selected with the semi-automatic procedure and the ones selected manually, respectively.

we first investigate possible selection / observational biases that might influence it.

We first investigate possible selection effects imposed by the semi-automatic procedure. Therefore we inspected all Fourier spectra by eye. We checked the Fourier spectra for excess power, as explained above, and were able to identify additional stars with power excess (blue symbols in Fig. 2). We identified more stars with oscillations at lower frequencies, where our semi-automatic procedure was truncated because of possible contamination with power excess due to granulation. In general these additional stars have a similar distribution of ν_{\max} as the ones selected with the semi-automatic procedure, see Fig. 4. Based on this, we discard the possibility that the peaked distribution is due to the identification method we used to select red giants with power excess due to solar-like oscillations.

In terms of observational biases, it is known that granulation is present in red-giant stars with power at low frequencies in the Fourier spectrum. In addition to the increase of granulation power, the width w of the oscillation power excess decreases with decreasing ν_{\max} , as this scales as $w \sim |\nu_{\max} - \nu_{ac}|$ (Kjeldsen & Bedding 1995). Both the increase of granulation and the smaller width of the power excess make it increasingly difficult to detect oscillations at low frequencies. Therefore the number of stars at low ν_{\max} is most likely underestimated.

To further investigate the low number of stars with $\nu_{\max} < 20 \mu\text{Hz}$, we checked whether stars with $\nu_{\max} < 20 \mu\text{Hz}$ lay in a specific part of the colour-magnitude diagram. In Fig. 5, the red-giant branch is shown with the stars for which we obtained ν_{\max} indicated in red, green and blue for stars with $\nu_{\max} < 20 \mu\text{Hz}$, stars with $20 \mu\text{Hz} \leq \nu_{\max} \leq 40 \mu\text{Hz}$ and stars with $\nu_{\max} > 40 \mu\text{Hz}$, respectively. Clearly, the stars with lowest ν_{\max} appear in the reddest and brightest part of the colour-magnitude diagram. This part of the colour-magnitude diagram is also less well populated, which decreases the probability of observing these stars. The low number of stars with $\nu_{\max} < 20 \mu\text{Hz}$ can therefore be explained by detection difficulties due to both granulation and decreasing width of the power excess, and low population density of stars with oscillations in this frequency range.

The decrease in the number of stars with ν_{\max} at frequencies $> 40 \mu\text{Hz}$ is partly caused by the fact that at higher fre-

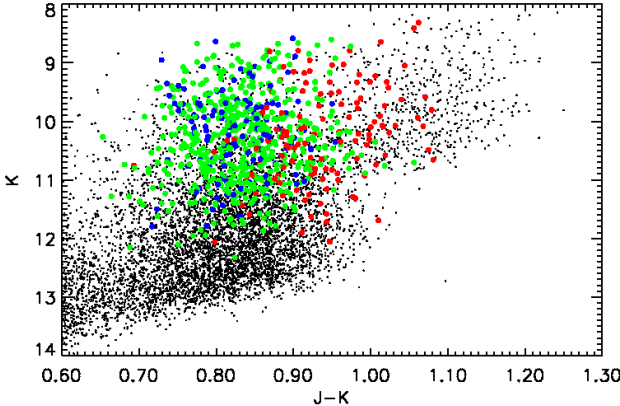


Fig. 5. The red giant branch of the colour-magnitude diagram as shown in Fig. 2. The black dots represent all targets in the field. Stars with $\nu_{max} < 20\mu\text{Hz}$, $20\mu\text{Hz} \leq \nu_{max} \leq 40\mu\text{Hz}$, $\nu_{max} > 40\mu\text{Hz}$ are indicated with red, green and blue dots respectively.

quencies the height of the power excess decreases, as can be seen in Fig. 3, and as is predicted by the scaling relations of Kjeldsen & Bedding (1995). When we look at the white noise (E in Eq. 1), whose values are shown as blue crosses in Fig. 3, we indeed see that at $\nu_{max} \sim 40\mu\text{Hz}$ the height of the oscillation power excess starts to decrease below the noise level of some stars with oscillations at lower frequencies. So for stars with $\nu_{max} > 40\mu\text{Hz}$ we can only detect solar-like oscillations for stars with low noise levels.

Naively, one would expect that the number of stars with a noise level below 100 ppm² would not depend on the frequency of maximum oscillation power. This would imply that we would be able to detect oscillations in a similar number of stars with these low noise levels irrespective of ν_{max} . Interestingly, the density of stars with a white noise level $\leq 100\text{ ppm}^2$ is much larger in the range $20\mu\text{Hz} \leq \nu_{max} \leq 40\mu\text{Hz}$ than at higher ν_{max} values, see the blue crosses in Fig. 3. This might again indicate that the population of observed stars with $\nu_{max} > 40\mu\text{Hz}$ is smaller than for stars with $20\mu\text{Hz} \leq \nu_{max} \leq 40\mu\text{Hz}$.

Population synthesis simulations to study the probability of observing a star at a certain position in the HR diagram are performed by Miglio et al. (2009). In their study, Miglio et al. (2009) simulate the composite stellar population of the observed field, using a population synthesis code that takes into account the morphology of the galaxy and star formation history. For further details we refer to Miglio et al. (2009) and references therein. The results for ν_{max} of these population synthesis simulations are in agreement with the observations presented here.

4.2. Large separation

A second interesting parameter is the large separation ($\Delta\nu$) between frequencies of modes with the same degree and consecutive overtones of the radial order. A theoretical investigation by Dupret et al. (2009) shows that the power spectra of the red-giant stars are different for different evolutionary phases. For more evolved stars only oscillations trapped in the outer cavity (p modes) can reach observable amplitudes at the surface of the star and for high-order low-degree modes these can show asymptotic, i.e., regular behaviour (Tassoul 1980). Other (less evolved) stars show a more dense and / or an irregular frequency pattern, which can be explained by the fact that the observed oscillations

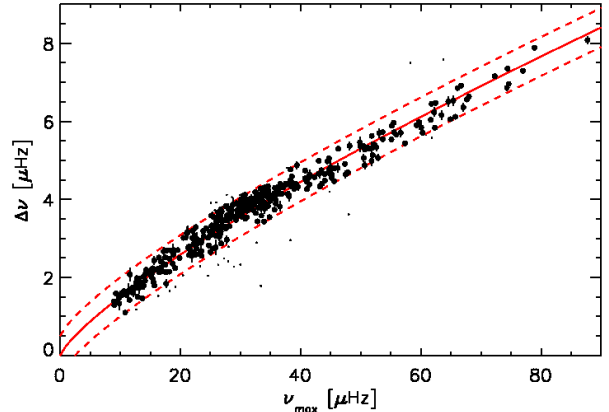


Fig. 6. $\Delta\nu$ as a function of ν_{max} , the small dots indicate $\Delta\nu$ values with a standard deviation $\leq 0.1\mu\text{Hz}$, but outside the $0.5\mu\text{Hz}$ interval (red dashed lines) around the correlation $\Delta\nu = \Delta\nu_\odot \cdot (\nu_{max}/\nu_{max_\odot})^{0.784\pm 0.003}$ (red solid line). The large dots are the 367 stars with $\Delta\nu$ values along the correlation and with standard deviation between the different measures $\leq 0.2\mu\text{Hz}$

are influenced by their behaviour in both the p-mode and g-mode cavity.

Due to the orbital frequencies of CoRoT at $\sim 163\mu\text{Hz}$ with several side lobes at $11.57\mu\text{Hz}$ intervals we were not able to investigate the less evolved stars at frequencies $150\text{--}200\mu\text{Hz}$ (model A, Dupret et al. 2009). Therefore, we expect to observe mainly more evolved stars for which theory predicts regular frequency patterns.

To study $\Delta\nu$, we first selected the frequency range in which we will compute $\Delta\nu$. This range is scaled from the Sun and defined as $\nu_{max} \pm 0.5 \cdot (\nu_{max}/\nu_{max_\odot}) \cdot w_\odot$, with w_\odot the width of the oscillation excess in the Sun. In this range, we compute the autocorrelation of the Fourier spectrum, the comb response function (Kjeldsen et al. 1995) and the autocorrelation of the time series (which is equivalent to the power spectrum of the power spectrum) (Roxburgh & Vorontsov 2006). For each of these methods we identified the highest peak as the possible $\Delta\nu$ (for the power spectrum of the power spectrum we assume $\Delta\nu/2$, see Roxburgh & Vorontsov (2006)). Then we computed the average $\Delta\nu$ and its standard deviation from the three values we obtained, taking the possibility that we identified $\Delta\nu/2$ or $2\Delta\nu$ into account. If one of the values is off by more than the standard deviation then it is excluded.

Resulting $\Delta\nu$ values with a standard deviation $\leq 0.1\mu\text{Hz}$ are considered to be more reliable and show a clear correlation with ν_{max} , see Fig. 6. This correlation follows the power law $\Delta\nu = \Delta\nu_\odot \cdot (\nu_{max}/\nu_{max_\odot})^{0.784\pm 0.003}$, which agrees well with the predictions and results of Stello et al. (2009) that have been made for solar-like main-sequence and sub-giant stars. All stars with a $\Delta\nu$ consistent with the described power law and additionally a standard deviation between the different measures $\leq 0.2\mu\text{Hz}$ are considered to have oscillation frequencies that occur at regular intervals.

Fig. 7 shows the fraction of stars in each ν_{max} bin for which we could determine $\Delta\nu$ as described above. With a two-sided Kolmogorov-Smirnov test (Press 2002), we find a 3% probability that the distribution is flat, i.e., that the fraction of stars for which we compute a reliable $\Delta\nu$ is the same for all ν_{max} bins. Nevertheless, there is no correlation present between the fraction of stars for which we obtain $\Delta\nu$ and ν_{max} . This is consistent with

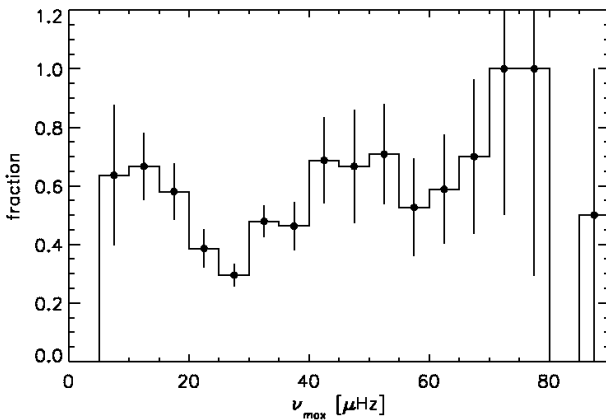


Fig. 7. Fraction of stars in each ν_{\max} interval for which we could determine $\Delta\nu$. The error bars are calculated assuming Poisson statistics (i.e., the fraction of stars for which we obtain $\Delta\nu$ divided by the square root of the number of stars for which we obtain $\Delta\nu$). Note that the dip in this distribution between 20 and 40 μHz coincides with most stars for which we obtained $\Delta\nu$ with at least two methods with a standard deviation $\leq 0.1 \mu\text{Hz}$, but which did not follow the power law, see the small dots in Fig. 6.

the theoretical models B, C, D and E of Dupret et al. (2009), for which regular frequency patterns are expected. The reason why we only detect $\Delta\nu$ for 367 stars might be due to noise / granulation peaks which could hamper the automatic determination. It might also be due to less well trapped $\ell = 1$ modes as predicted by Dupret et al. (2009) for stars intermediate in the red giant branch. Furthermore, in the scaling relation used here, no dependence on stellar parameters is included.

We note here that for an additional 303 stars a value for $\Delta\nu$ within the 0.5 μHz interval around the correlation could be obtained with only one of the methods. Including these less reliable values in the fraction of stars in each ν_{\max} interval sustains the conclusion that no correlation is present between the fraction of stars for which we determine $\Delta\nu$ and ν_{\max} in the frequency range considered here.

5. Summary and Conclusions

We were able to detect power excess resembling solar-like oscillations in 778 stars observed in the CoRoT exofield LRC01 at frequencies typical for solar-like oscillations in red (G-K) giants. These detections were made with a semi-automatic procedure with which we were able to detect oscillation power excess for the brightest stars at frequencies $> 20 \mu\text{Hz}$. For fainter stars, with a less pronounced power excess, and more luminous stars, with an excess at lower frequencies, the semi-automatic procedure was less successful and an inspection by eye is performed to investigate the presence of red-giant stars with solar-like oscillations in these frequency regimes.

This large number of detections increases the number of red-giant stars with observed solar-like oscillations by a factor of 100 and allows for a statistical investigation into the general properties of these stars.

From the distribution of ν_{\max} , it becomes clear that it is most likely to observe red giants with oscillation power between 20 and 40 μHz . Apart from the fact that we suffer from biases due to granulation / decreasing width of the oscillation excess at low frequencies and white noise at high frequencies, the increase /

decrease in the number of stars with ν_{\max} is also influenced by a varying population density. Evidence for this conclusion is also demonstrated by population synthesis studies, for which we refer to Miglio et al. (2009).

For about half of the stars (367) we could obtain consistent values for $\Delta\nu$ with at least two methods. These values follow the power law $\Delta\nu \sim (\nu_{\max})^{0.784 \pm 0.003}$. A similar result has already been found for solar-like main-sequence and subgiant stars (Stello et al. 2009). This correlation is equivalent with $\Delta\nu \sim c_s/R \sim (c_s/H_p)^{0.784 \pm 0.003}$, where c_s is the sound speed, R the radius and H_p the pressure scale height of the atmosphere (Kjeldsen & Bedding 1995). From the fact that this relation holds for both solar-like stars and red giants, we conclude that the sound travel time over the pressure scale height of the atmosphere scales with the sound travel time through the whole star in the same way in both evolutionary states.

Furthermore, we find that the fraction of stars for which we obtain a regular spectrum varies in a complicated way with ν_{\max} in the frequency range up to 100 μHz . This is in agreement with the predictions by Dupret et al. (2009) as we observe mainly stars intermediate or high in the red giant branch. For these stars modes trapped in the outer cavity can reach observational amplitudes and for high-order low-degree modes the frequencies will follow the asymptotic relation (Tassoul 1980).

The results obtained for red giants with CoRoT are important for improving our understanding of solar-like oscillations in red-giant stars. These observations allow us to study, for instance, the excitation and damping of these oscillations and the time scales at which these processes occur. Studying these parameters as a function of evolution will also be possible with the large number of red giants showing oscillations. Furthermore, non-radial modes with long lifetimes (De Ridder et al. 2009) open a way to study the internal structure of individual giants in detail. These studies are currently underway.

Acknowledgements. SH wants to thank W.J. Chaplin for useful discussions and A.-M. Broomhall for carefully reading the manuscript. SH acknowledges financial support from the Belgian Federal Science Policy (ref: MO/33/018). TK and WWW acknowledges support by the Austrian Research Promotion Agency (FFG), and the Austria Science Fund (FWF P17580). FC is a postdoctoral fellows of the Fund for Scientific Research Flanders. APH acknowledges the support of grant 500W0204 from the Deutsches Zentrum für Luft- und Raumfahrt e. V. (DLR). We would like to thank our referee T.R. Bedding for valuable comments, which helped to improved the manuscript considerably.

References

- Aigrain, S., Favata, F., & Gilmore, G. 2004, A&A, 414, 1139
- Auvergne, M., Bodin, P., Boisnard, L., et al. 2009, ArXiv e-prints
- Baglin, A. & Chaintreuil, S. 2006, in ESA Special Publication, Vol. 1306, ESA Special Publication, ed. M. Fridlund, A. Baglin, J. Lochard, & L. Conroy, 279
- Bessell, M. S. & Brett, J. M. 1988, PASP, 100, 1134
- Brown, T. M., Gilliland, R. L., Noyes, R. W., & Ramsey, L. W. 1991, ApJ, 368, 599
- Chaplin, W. J., Houdek, G., Karoff, C., Elsworth, Y., & New, R. 2009, ArXiv e-prints
- De Ridder, J., Barban, C., Baudin, F., et al. 2009, Nature, 459, 398
- Debosscher, J., Sarro, L. M., Aerts, C., et al. 2007, A&A, 475, 1159
- Deleuil, M., Moutou, C., Deeg, H. J., et al. 2006, in ESA Special Publication, Vol. 1306, ESA Special Publication, ed. M. Fridlund, A. Baglin, J. Lochard, & L. Conroy, 341
- Dupret, M.-A., Belkacem, K., Samadi, R., et al. 2009, submitted
- Kallinger, T., Weiss, W. W., Barban, C., et al. 2009, A&A, submitted
- Kjeldsen, H. & Bedding, T. R. 1995, A&A, 293, 87
- Kjeldsen, H., Bedding, T. R., Arentoft, T., et al. 2008, ApJ, 682, 1370
- Kjeldsen, H., Bedding, T. R., Viskum, M., & Frandsen, S. 1995, AJ, 109, 1313
- Miglio, A., Montalbán, J., Baudin, F., et al. 2009, A&A, submitted

- Press, W. H. 2002, Numerical recipes in C++ : the art of scientific computing (Numerical recipes in C++ : the art of scientific computing by William H. Press. xxviii, 1.002 p. : ill. ; 26 cm. Includes bibliographical references and index. ISBN : 0521750334)
- Roxburgh, I. W. & Vorontsov, S. V. 2006, MNRAS, 369, 1491
- Stello, D., Chaplin, W. J., Basu, S., & Elsworth, Y. P. 2009, A&A, in prepartion
- Tassoul, M. 1980, ApJS, 43, 469

Table 1. Red giant candidates selected in the CoRoT exofield during run LRc01: CoRoT identification number (CoRoT-ID), apparent magnitude (m_v), right ascension (ra) in degrees, declination (dec) in degrees, frequency of maximum oscillation power (ν_{max}) and large separation ($\Delta\nu$) in μ Hz when obtained, see text. The $\Delta\nu$ values between () are values which follow the $\Delta\nu \sim \nu_{max}^{0.784 \pm 0.003}$ relation but are only obtained with one method. 'sap' means that a star is selected with a semi-automatic procedure and 'man' means that the star is selected by eye only.

CoRoT-ID	m_v	ra (degrees)	dec (degrees)	ν_{max} (μ Hz)	$\Delta\nu$ (μ Hz)	classification
100411979	14.875	290.58484	1.69915	29.7	(3.6)	man
100440565	13.149	290.62716	1.64784	29.1	3.6	sap
100475529	13.574	290.67846	1.78820	32.3	3.9	sap
100482282	14.125	290.68833	1.72073	13.1	1.7	man
100483847	12.700	290.69070	1.52023	39.1	4.4	sap
100486326	13.465	290.69441	1.40077	10.0	(1.7)	man
100497523	12.684	290.71066	1.40175	34.2		sap
100500736	14.041	290.71553	1.37232	30.7	4.1	sap
100502521	15.330	290.71812	1.47512	28.6	(3.6)	man
100503016	14.278	290.71883	1.33593	10.9	(1.5)	man
100503737	14.414	290.71987	1.42503	25.7	(2.9)	man
100511611	14.340	290.73162	1.64333	11.5	1.6	man
100515307	14.795	290.73734	1.72422	26.7	3.7	man
100516923	14.975	290.73967	1.81010	45.9	(4.7)	man
100516924	14.221	290.73967	1.34772	38.6	4.4	man
100518590	14.590	290.74216	1.45303	34.0		man
100520462	14.368	290.74493	1.33203	14.1	1.9	man
100523200	13.359	290.74899	1.48020	15.7	1.8	man
100525640	14.941	290.75262	1.59460	31.2	(3.9)	sap
100528464	13.405	290.75684	1.63503	14.3	2.2	man
100530452	13.649	290.75968	1.28913	35.8	4.0	sap
100545483	12.724	290.78246	1.49500	61.6	6.0	sap
100546715	15.318	290.78436	1.59082	28.1	(3.3)	man
100552455	14.274	290.79288	1.51853	63.0	(6.1)	man
100555173	12.394	290.79705	1.31657	31.4	(3.7)	sap
100556001	12.540	290.79836	1.59940	45.2	4.6	sap
100556055	13.199	290.79845	1.84249	44.8	(4.8)	sap
100556225	14.388	290.79873	1.55524	27.3	(3.6)	man
100562083	13.969	290.80760	1.82471	41.5	4.6	man
100564275	14.494	290.81101	1.75957	34.4	(4.0)	sap
100573220	13.259	290.82440	1.83611	33.3	4.3	sap
100586764	14.155	290.84463	1.47716	25.2	(3.3)	sap
100591536	14.604	290.85186	1.06328	35.5	(4.4)	man
100591900	14.030	290.85235	1.63926	37.8		man
100592544	13.690	290.85334	1.69705	44.0	4.5	sap
100593268	13.339	290.85442	1.26642	29.6	(3.3)	sap
100593396	13.554	290.85460	1.47886	45.6	4.5	sap
100596299	14.920	290.85899	1.75909	40.7	4.5	man
100597075	13.749	290.86020	1.29505	12.7	1.8	man
100597609	13.024	290.86096	1.45091	36.6	3.8	sap
100598266	14.609	290.86194	1.77280	9.3	1.6	man
100602088	14.373	290.86763	1.02124	30.2	3.8	sap
100605342	14.040	290.87237	1.30235	27.3		man
100606331	13.733	290.87381	1.31963	23.4	2.9	man
100614937	14.668	290.88591	1.47120	27.5	(2.8)	man
100615971	13.160	290.88742	1.87220	32.5	3.6	sap
100630893	12.990	290.90775	1.76520	27.8	(3.4)	sap
100637413	13.150	290.91673	1.87779	28.3	(3.1)	sap
100644163	13.375	290.92629	1.46415	38.2	(4.6)	sap
100652335	14.547	290.93765	1.70149	23.4	2.9	man
100652396	16.049	290.93775	1.46657	19.3	(2.7)	man
100654821	12.632	290.94131	1.89830	31.7	(3.8)	sap
100657953	14.573	290.94618	1.55220	15.2	2.1	man
100662481	12.898	290.95388	1.38109	50.7	4.9	sap
100667041	15.216	290.96172	1.19518	19.1	2.2	man
100667742	15.506	290.96290	1.16010	32.7	(4.1)	man
100678257	14.681	290.98050	1.26305	25.6		man
100678505	12.198	290.98093	1.67693	64.3	(6.4)	man

Table 1. continued.

CoRoT-ID	m_v	ra (degrees)	dec (degrees)	ν_{max} (μ Hz)	$\Delta\nu$ (μ Hz)	selection
100679411	14.681	290.98248	1.29397	25.5	3.6	man
100682488	13.691	290.98765	1.17854	50.5	5.1	sap
100688417	14.113	290.99775	1.61537	19.1	(2.5)	man
100688591	13.708	290.99806	1.54563	35.8		sap
100697490	12.541	291.01319	1.84065	60.9	(5.7)	sap
100698309	13.648	291.01460	1.54950	16.4		man
100705263	14.241	291.02636	0.96980	35.6	4.1	sap
100707942	14.521	291.03102	1.27638	62.8	(6.3)	man
100714007	14.032	291.04135	1.83044	27.4	(3.4)	sap
100714474	13.815	291.04208	1.52403	36.2	4.1	sap
100716817	13.858	291.04621	1.63556	35.0	4.0	sap
100722680	14.991	291.05657	1.05631	12.8	2.0	man
100724563	13.601	291.06068	1.68904	10.3	1.5	man
100725658	14.635	291.06352	1.77049	22.0	3.0	man
100729865	13.806	291.07170	1.13569	26.1	3.3	man
100733133	13.624	291.07624	0.58899	34.7	(3.8)	sap
100733870	14.204	291.07717	0.88983	30.9	3.9	sap
100736020	12.623	291.08004	1.64963	34.8	3.5	sap
100736789	13.046	291.08107	1.19551	9.7	(1.8)	man
100737490	14.486	291.08209	0.69028	13.0	1.8	man
100738231	14.643	291.08303	1.50924	27.6	3.3	sap
100738670	14.847	291.08363	1.90112	29.7	3.7	man
100742554	14.628	291.08879	1.76733	19.2		man
100743629	14.043	291.09024	1.63491	27.6		man
100745423	12.873	291.09263	1.75048	12.5	1.7	man
100747150	14.378	291.09483	0.83749	18.4	2.7	man
100752538	12.618	291.10197	1.89511	35.5	(4.1)	sap
100758194	14.191	291.10964	1.70849	26.6	3.6	sap
100758361	14.385	291.10991	1.40466	29.9		man
100763478	13.192	291.11677	1.58127	32.4	(3.7)	sap
100768145	13.163	291.12307	1.81926	38.6	(4.4)	sap
100770682	14.266	291.12658	1.14876	26.7	(2.7)	man
100773163	13.901	291.12987	1.10874	46.3	5.3	sap
100782155	13.141	291.14165	1.11360	57.4	5.4	sap
100784138	14.198	291.14421	1.68746	26.6	3.3	man
100787298	14.936	291.14853	1.14182	28.4	3.7	man
100790731	13.846	291.15304	1.17988	31.9	(3.6)	sap
100790822	15.203	291.15315	1.47807	9.1	(1.5)	man
100790832	14.226	291.15317	0.77703	57.4	(5.7)	sap
100792637	12.883	291.15562	1.82894	52.9	5.1	man
100793294	14.276	291.15646	0.71483	34.7	4.1	sap
100795824	12.967	291.15980	1.89581	38.3	4.8	man
100799833	12.183	291.16502	1.68434	33.0	3.8	sap
100802610	14.893	291.16867	0.37907	29.9		man
100805172	13.181	291.17204	1.57948	32.1	3.7	sap
100807132	14.480	291.17456	1.84306	31.5		man
100809477	15.081	291.17756	0.96286	31.3	3.8	man
100809880	13.967	291.17808	1.99645	67.1	6.4	man
100813027	15.011	291.18237	0.94779	25.0	(3.3)	man
100813221	15.773	291.18264	1.69099	10.0	1.5	man
100813661	14.298	291.18322	1.60183	27.9	(3.6)	man
100813799	13.756	291.18340	1.35718	65.7	6.1	man
100817208	14.083	291.18790	1.60311	48.2	5.4	man
100819874	12.571	291.19141	1.59430	24.3	3.3	sap
100820820	14.621	291.19264	1.22416	11.6	2.1	man
100821572	13.969	291.19365	1.33072	53.2		man
100824618	14.781	291.19754	1.51247	11.5	1.4	man
100826011	15.096	291.19939	1.84490	50.1		man
100826123	14.713	291.19953	1.46327	40.4	(4.1)	man
100826589	13.366	291.20015	1.27822	27.7	3.5	sap
100827073	14.331	291.20081	0.93753	34.0	3.8	sap

Table 1. continued.

CoRoT-ID	m_v	ra (degrees)	dec (degrees)	ν_{max} (μ Hz)	$\Delta\nu$ (μ Hz)	selection
100827490	13.453	291.20139	1.66865	15.0	(2.0)	man
100828924	14.516	291.20327	1.15196	18.2		man
100830101	14.552	291.20477	0.32313	26.5	3.0	sap
100833997	13.806	291.20989	0.65472	31.4	3.9	sap
100834084	12.548	291.21001	1.64546	31.8	4.0	sap
100836428	14.242	291.21317	1.94311	31.6	4.0	sap
100836619	14.229	291.21345	0.45605	28.0	(3.7)	sap
100837771	13.696	291.21496	1.29365	38.8	(4.2)	sap
100838216	14.361	291.21550	0.99303	37.8	4.1	man
100838545	12.758	291.21593	1.49494	29.5	(3.7)	sap
100841360	13.452	291.21953	1.95018	20.5	3.0	sap
100841417	14.014	291.21961	0.43728	18.8	2.6	man
100845030	14.456	291.22450	0.63361	30.6	3.9	sap
100845233	13.688	291.22475	1.62023	28.5	(3.0)	man
100846057	12.260	291.22584	1.54956	28.3	(3.3)	sap
100849897	14.334	291.23092	0.46696	59.7	5.9	sap
100852459	14.206	291.23427	1.58504	29.1	(3.5)	man
100853452	12.629	291.23553	0.52005	32.3		sap
100853745	13.779	291.23586	1.56867	39.7	(4.6)	man
100855073	14.133	291.23768	1.51050	26.5		sap
100856144	14.108	291.23909	1.36622	37.9		man
100856234	13.359	291.23923	0.41364	102.4	(8.9)	man
100856697	14.214	291.23982	0.87455	47.4	4.9	man
100858245	13.742	291.24183	0.27329	31.5	(3.2)	sap
100861153	14.596	291.24562	0.75779	36.9	4.1	man
100861203	14.532	291.24569	0.21613	28.9	(3.8)	man
100861335	13.042	291.24587	0.20847	34.8	4.1	sap
100864569	13.254	291.25008	0.44017	63.7		man
100867373	15.447	291.25370	1.91347	24.6	(3.2)	man
100867895	13.712	291.25435	1.92338	33.9	(3.9)	sap
100868399	14.032	291.25501	1.95535	14.3	(2.2)	man
100871490	14.951	291.25914	1.13485	27.6	(3.5)	man
100872561	15.537	291.26063	1.93630	12.7	(1.9)	man
100873140	14.436	291.26135	0.75795	26.7	3.5	man
100873731	13.641	291.26206	1.01897	35.2	(3.8)	sap
100879189	14.548	291.26935	1.68646	23.1	(3.3)	man
100880990	12.138	291.27175	1.61755	32.2	3.9	sap
100885791	14.609	291.27815	1.33483	32.2	3.9	sap
100886873	13.571	291.27959	1.10133	40.8	4.7	sap
100886908	14.404	291.27965	0.42005	10.8	1.1	man
100887322	13.337	291.28018	0.23459	40.2		man
100887322	13.337	291.28018	0.23459	40.3		sap
100888944	14.312	291.28229	0.23944	48.0		man
100889852	14.630	291.28348	1.87466	53.0	(5.6)	man
100892148	13.813	291.28663	1.78360	55.1	5.5	man
100893246	14.806	291.28800	1.21694	32.2	(3.8)	man
100893803	14.746	291.28877	1.85592	33.5	3.6	man
100896955	14.831	291.29285	1.20868	26.3		man
100898422	12.583	291.29480	1.67532	37.5	4.4	sap
100899564	14.779	291.29634	1.54729	16.4	(2.6)	man
100900153	13.616	291.29703	1.14535	27.2		sap
100901855	14.174	291.29931	0.84220	25.2	3.3	man
100901998	12.501	291.29949	0.94324	47.5	4.6	sap
100902585	15.029	291.30027	0.41639	27.4	(2.9)	man
100905864	14.037	291.30457	1.99818	30.0	(3.9)	man
100908597	13.949	291.30820	0.56744	29.4	3.7	sap
100911685	13.393	291.31240	2.01897	23.8	3.1	man
100911815	12.959	291.31260	0.47401	22.6	3.3	sap
100914315	14.419	291.31597	0.56954	35.4		man
100914473	15.222	291.31617	0.21228	16.4	2.2	man
100915882	14.766	291.31813	1.18749	29.5	(3.5)	man

Table 1. continued.

CoRoT-ID	m_v	ra (degrees)	dec (degrees)	ν_{max} (μ Hz)	$\Delta\nu$ (μ Hz)	selection
100920975	14.528	291.32494	1.77388	12.8	(2.0)	man
100921071	13.993	291.32506	1.73479	29.3	(3.7)	sap
100921343	12.914	291.32543	0.36513	30.5	3.8	sap
100922068	14.447	291.32638	0.10787	26.5	(3.4)	man
100922474	14.057	291.32692	0.28199	29.3	(3.7)	man
100922926	12.896	291.32753	0.01955	31.0	3.5	sap
100923801	14.074	291.32866	0.42331	32.8		sap
100924078	13.267	291.32901	0.37681	17.4	(2.4)	sap
100928979	13.007	291.33535	0.02051	35.7	4.3	sap
100929178	14.710	291.33565	1.85446	12.0	1.7	man
100929688	13.046	291.33638	1.32690	13.9	1.8	man
100934222	14.121	291.34249	1.51435	36.7	(3.9)	man
100935924	14.806	291.34490	1.33433	37.3		man
100937183	13.632	291.34659	0.24906	34.0	(4.0)	sap
100937360	14.283	291.34683	1.50686	25.1	3.6	man
100940297	13.947	291.35072	0.15197	66.1	6.9	man
100943381	13.383	291.35483	0.37929	15.6	1.9	man
100945495	13.189	291.35774	0.45517	32.3	(4.0)	sap
100948410	15.182	291.36163	1.98400	26.5	(3.2)	man
100949965	14.200	291.36378	1.82220	11.0	1.5	man
100953642	13.271	291.36866	0.87465	17.4	(2.5)	sap
100954989	13.974	291.37053	1.50879	33.8	(4.2)	sap
100956384	14.466	291.37237	0.80213	32.8	(3.8)	sap
100958423	14.762	291.37519	0.35152	11.4	1.7	man
100958571	14.660	291.37535	1.00666	14.5	2.2	man
100958710	12.477	291.37553	0.08861	33.5	(4.0)	sap
100959121	13.002	291.37607	2.02423	33.9	3.9	sap
100960341	14.766	291.37768	1.27744	43.7		man
100967582	14.060	291.38714	2.01422	20.7	(2.9)	man
100968429	13.774	291.38827	1.35596	31.5	(3.7)	sap
100968875	13.666	291.38887	1.32535	25.0	2.6	man
100971166	14.262	291.39191	1.15215	15.2	2.0	man
100971567	14.177	291.39248	1.77656	11.6	(1.6)	man
100971774	13.651	291.39272	1.50388	52.2	5.4	man
100973808	13.594	291.39547	1.43117	32.8		sap
100974118	13.744	291.39585	0.36911	39.1		sap
100980762	13.466	291.40460	1.96770	28.7		man
100981445	14.328	291.40551	1.38470	30.1	3.9	man
100983148	13.601	291.40783	0.92724	33.9	3.4	sap
100983871	13.514	291.40879	1.69909	38.0	4.1	sap
100985849	13.713	291.41140	1.94710	34.7		sap
100986828	14.430	291.41277	1.79596	31.8	(4.0)	man
100988199	14.296	291.41463	0.73395	28.1	3.6	man
100988656	15.149	291.41524	0.51981	18.6	(2.1)	man
100988725	13.274	291.41532	1.69215	26.1	3.4	sap
100988784	14.415	291.41540	0.20058	58.5	(5.8)	man
100988877	14.429	291.41553	1.24339	36.0	(3.6)	sap
100989736	14.811	291.41675	0.95345	30.8	(4.0)	man
100991403	14.502	291.41892	0.43622	26.5	(3.0)	man
100991658	13.055	291.41925	1.38877	50.7	5.3	sap
100992435	14.320	291.42033	1.78134	28.0	(2.8)	man
100993976	13.380	291.42232	0.98060	22.4	(3.2)	sap
100994184	15.579	291.42260	1.56377	13.1	(1.3)	man
100997312	15.230	291.42682	0.94810	18.2	2.5	man
100998571	13.704	291.42852	-0.20099	23.5	2.9	sap
101000321	12.780	291.43091	0.60447	39.4	4.9	sap
101001054	12.848	291.43183	0.46790	38.9	4.3	sap
101002050	13.274	291.43318	-0.25271	24.9	3.2	sap
101004170	14.752	291.43612	-0.08080	42.8	(4.3)	man
101005339	14.186	291.43780	1.89714	29.0	(3.6)	man
101009305	13.590	291.44377	0.45081	9.7	1.5	man

Table 1. continued.

CoRoT-ID	m_v	ra (degrees)	dec (degrees)	ν_{max} (μ Hz)	$\Delta\nu$ (μ Hz)	selection
101009538	14.167	291.44420	1.46534	32.7		man
101015137	14.840	291.45425	0.95231	44.8	4.7	man
101015642	14.417	291.45515	0.15252	25.4	(3.2)	man
101016219	14.007	291.45625	0.18111	36.3	(4.0)	sap
101017465	14.092	291.45850	0.23151	9.0	1.3	man
101017915	15.065	291.45932	2.12550	21.0	(2.8)	man
101018056	15.042	291.45955	0.13176	24.4	(3.1)	man
101018393	13.982	291.46019	-0.02272	16.4	2.5	man
101019013	13.906	291.46139	-0.31073	41.1	4.3	man
101020804	14.391	291.46472	-0.18978	67.0		man
101021652	13.677	291.46630	1.41317	28.6	(3.7)	sap
101022193	13.245	291.46728	2.09455	34.6	(4.0)	sap
101023768	13.942	291.47014	0.21349	41.4	4.6	man
101023918	14.111	291.47042	-0.26929	44.4	5.0	man
101024376	12.797	291.47122	0.04472	18.2	(2.6)	sap
101025128	14.415	291.47269	1.90547	32.9	3.4	sap
101025264	14.572	291.47295	0.21938	20.4	(2.2)	man
101025358	13.902	291.47314	0.24386	29.4		sap
101025964	14.892	291.47426	0.28930	55.7	(5.9)	man
101026664	14.486	291.47558	1.33582	51.8	5.0	man
101027968	12.787	291.47797	0.53973	40.9	4.5	sap
101029591	13.851	291.48099	-0.27215	28.5	(3.0)	man
101030924	14.397	291.48348	0.62523	69.3	(6.2)	man
101032580	12.783	291.48659	1.11159	43.5	4.4	sap
101033184	14.905	291.48775	1.91896	17.1	2.2	man
101034439	13.955	291.49014	2.00285	29.5	(3.8)	man
101034839	14.547	291.49086	0.19576	9.9	1.5	man
101034881	13.500	291.49093	0.93401	43.5	4.7	sap
101035230	13.628	291.49162	0.83570	46.9	(5.1)	sap
101035304	13.195	291.49178	2.03472	24.0		sap
101035766	12.906	291.49261	1.31397	10.2	1.5	man
101037083	13.390	291.49512	1.59448	39.1		sap
101039409	13.695	291.49944	2.06531	34.8		sap
101039834	14.775	291.50017	2.07042	29.2	3.5	man
101040751	15.037	291.50194	1.51269	11.5	(1.1)	man
101041814	13.507	291.50399	1.52722	43.0	5.0	sap
101042011	13.115	291.50433	2.04700	34.3	(3.4)	sap
101043587	12.202	291.50727	0.55733	45.9	(4.6)	man
101044584	12.996	291.50928	-0.31709	25.2	(3.3)	sap
101044694	15.106	291.50948	1.28669	18.1	2.1	man
101044836	13.142	291.50975	-0.08486	12.8	(1.4)	man
101045095	13.967	291.51019	0.06251	21.3	2.8	man
101046542	14.972	291.51296	0.55712	16.4	(2.3)	man
101046557	13.265	291.51298	2.16556	61.8	6.5	sap
101046788	14.392	291.51342	0.16831	22.1	3.2	man
101047228	13.547	291.51423	1.40513	51.8	5.6	sap
101050198	14.250	291.51984	1.56576	25.0	(3.2)	man
101050222	13.281	291.51988	-0.27829	47.9	4.7	sap
101050462	14.495	291.52036	1.63532	28.5		man
101050632	13.947	291.52068	0.47317	28.3	3.8	sap
101051096	13.753	291.52161	1.70241	31.5	(3.1)	sap
101054647	14.168	291.52828	0.87295	51.9	5.3	sap
101056009	13.917	291.53086	1.44659	24.3	(3.0)	sap
101056429	15.087	291.53170	0.61065	60.3		man
101057165	14.067	291.53303	0.10175	18.4	(2.5)	man
101057962	12.691	291.53458	-0.42275	13.0	(2.1)	man
101058180	12.613	291.53505	1.86233	31.2	3.9	sap
101058880	13.680	291.53638	1.56013	43.2	4.3	sap
101059151	13.353	291.53683	1.72685	26.7	(3.5)	sap
101059381	12.622	291.53722	-0.00047	30.1	3.9	sap
101061858	13.995	291.54200	2.17327	25.5	(3.1)	man

Table 1. continued.

CoRoT-ID	m_v	ra (degrees)	dec (degrees)	ν_{max} (μ Hz)	$\Delta\nu$ (μ Hz)	selection
101062545	13.015	291.54330	2.15023	36.6	4.4	sap
101063559	13.682	291.54524	-0.03343	20.6	(2.3)	sap
101064543	14.187	291.54719	-0.10572	38.3	4.5	sap
101064646	14.797	291.54739	1.52595	37.8	(4.5)	man
101065131	14.497	291.54832	0.67604	24.9	(2.9)	man
101065685	14.915	291.54940	1.55568	25.9	3.3	man
101066347	13.847	291.55069	1.45060	55.9	5.7	man
101067603	13.520	291.55316	0.84204	31.9	3.9	sap
101069862	14.084	291.55770	1.82206	30.1		sap
101071139	15.535	291.56076	2.12895	25.4	(3.3)	man
101071751	13.951	291.56292	-0.22354	13.4	(1.5)	man
101072055	15.027	291.56414	1.47770	23.2	(2.6)	man
101073282	14.010	291.56788	1.27910	56.6	(5.6)	man
101073867	14.487	291.56904	0.67811	30.0	3.7	sap
101077806	14.161	291.57535	1.33321	27.9	(3.0)	sap
101078244	13.879	291.57602	2.08795	35.9	3.9	sap
101079646	14.556	291.57824	1.84024	67.6	6.6	man
101080756	13.850	291.58006	0.38919	55.5	6.0	man
101081290	12.731	291.58092	-0.54983	51.1	5.3	sap
101084795	14.079	291.58641	0.58372	23.3		man
101085186	14.753	291.58706	1.25963	34.0	(3.7)	man
101087560	14.368	291.59076	0.04236	26.3	(2.9)	man
101090302	15.298	291.59503	-0.16770	31.5	(3.8)	man
101090411	12.938	291.59520	1.85245	27.1	(3.7)	sap
101090725	14.985	291.59567	0.88635	19.5		man
101092562	14.238	291.59859	0.04762	16.9	(2.3)	man
101092813	12.032	291.59895	-0.05994	33.7	(3.4)	sap
101093482	14.280	291.60003	1.60977	77.0	7.3	man
101093867	14.150	291.60058	1.68520	27.5		man
101094148	13.985	291.60098	2.02947	21.4	2.6	sap
101098439	13.631	291.60761	1.04801	27.9	(3.6)	sap
101098782	12.672	291.60819	0.24737	20.6	(2.4)	sap
101099173	12.733	291.60879	1.95501	22.4	3.1	man
101099720	12.906	291.60964	-0.21804	34.2	4.1	sap
101100065	13.274	291.61023	0.49958	34.9	4.1	sap
101100415	14.877	291.61082	0.16362	27.1	(2.7)	man
101101232	13.889	291.61213	2.05483	30.1	(3.7)	sap
101101253	14.289	291.61217	1.54975	12.5	(2.1)	man
101102567	14.031	291.61426	-0.48679	15.7	2.2	man
101103214	12.914	291.61532	2.01659	26.3	3.2	sap
101106018	14.005	291.61961	2.19416	29.9	(3.6)	sap
101106220	14.642	291.61992	0.21139	26.2	(3.4)	man
101107208	13.082	291.62149	0.19295	32.3	4.0	sap
101108197	13.826	291.62301	-0.35573	17.8	2.7	man
101108258	15.059	291.62312	-0.62965	24.6	(2.9)	man
101108472	15.037	291.62346	0.13823	34.3	(3.4)	man
101111723	13.828	291.62856	1.06470	36.2	(4.2)	man
101111963	13.605	291.62890	2.14874	17.5	2.5	man
101112259	13.769	291.62938	1.57138	60.3	5.7	man
101113062	13.462	291.63062	-0.03739	72.3	7.2	sap
101114620	14.725	291.63303	2.13688	28.3	(3.8)	man
101115198	15.121	291.63398	-0.39851	45.0	4.8	man
101116845	14.038	291.63650	1.03435	37.7	(4.5)	sap
101118040	14.152	291.63838	0.16601	26.5		man
101119005	14.165	291.63994	0.59070	66.7	6.9	man
101120312	14.939	291.64210	1.97412	27.4	3.5	man
101121241	14.653	291.64349	2.01468	30.1	3.8	man
101122421	12.824	291.64539	0.38612	43.1	4.7	sap
101123395	12.939	291.64689	2.04155	46.3	(4.7)	sap
101123432	13.488	291.64696	1.24289	26.2		sap
101124344	13.176	291.64837	-0.45699	37.6	(4.2)	sap

Table 1. continued.

CoRoT-ID	m_v	ra (degrees)	dec (degrees)	ν_{max} (μ Hz)	$\Delta\nu$ (μ Hz)	selection
101126093	15.401	291.65111	-0.58210	15.4	2.2	man
101126186	15.095	291.65127	1.56076	27.0	3.3	man
101127623	13.652	291.65358	0.54981	35.1	(3.5)	man
101130130	13.343	291.65749	1.25378	15.6	(2.2)	man
101133310	14.504	291.66246	1.97811	39.6	4.3	sap
101134441	14.500	291.66421	1.68784	39.0	4.4	sap
101136306	12.611	291.66706	1.45305	30.8	4.0	sap
101137245	14.115	291.66853	2.10456	27.4	(3.3)	sap
101139228	12.559	291.67170	-0.63344	30.2	3.6	sap
101141206	14.242	291.67469	1.58847	22.5	(3.0)	man
101141309	13.387	291.67488	0.29601	9.8	1.3	man
101141846	14.017	291.67575	0.20753	29.5		sap
101144124	14.375	291.67935	2.23243	27.9		man
101144866	14.694	291.68057	0.32887	15.1	2.2	man
101145517	14.108	291.68161	1.23084	29.6		man
101147664	14.885	291.68493	1.64543	33.6	(3.5)	man
101148382	13.473	291.68605	1.70738	34.6	(4.2)	sap
101149674	14.756	291.68817	1.86692	24.6	(3.3)	man
101150004	12.505	291.68868	2.22050	28.6	3.5	sap
101150212	13.885	291.68899	1.77616	25.1		man
101150411	14.240	291.68926	0.50928	26.3	(3.0)	man
101150783	14.482	291.68987	1.85087	21.9	2.6	man
101150795	14.108	291.68989	0.86599	25.2	3.2	sap
101151242	14.018	291.69058	1.14597	42.8	(4.2)	man
101151570	15.292	291.69110	0.28046	12.7	1.8	man
101154362	13.131	291.69547	-0.20668	29.4	3.6	sap
101154828	13.622	291.69617	0.14189	16.8	2.3	man
101162331	14.142	291.70800	-0.09266	25.9	(3.3)	man
101162392	12.718	291.70811	1.19743	45.6	4.8	sap
101162838	14.798	291.70884	1.86259	23.9		man
101163504	13.951	291.70989	0.02366	74.6	7.0	man
101163959	13.971	291.71061	1.07502	28.7	(3.5)	man
101164110	13.705	291.71085	2.19214	26.9	(3.7)	man
101164298	14.457	291.71114	0.31052	26.6		man
101165983	13.551	291.71389	-0.19336	34.6	4.3	sap
101166514	15.721	291.71474	-0.29253	27.7	3.6	man
101166955	14.778	291.71538	1.27191	10.5	(1.0)	man
101167637	13.037	291.71646	0.73351	33.4	3.9	man
101167976	15.455	291.71698	2.18577	33.5	3.9	man
101169312	13.858	291.71908	0.88646	28.5	(3.3)	man
101169337	14.554	291.71912	1.09439	53.7	5.5	man
101169641	15.301	291.71956	-0.55280	28.0	3.8	man
101171937	14.205	291.72328	1.55262	33.4		sap
101172152	14.127	291.72359	0.60772	30.4	3.7	sap
101172950	14.204	291.72483	1.95543	27.1	3.3	man
101173044	12.527	291.72497	0.19681	35.1	(4.4)	sap
101174701	14.907	291.72757	0.28982	26.3	3.7	man
101175503	13.660	291.72881	0.45476	26.2	(3.1)	sap
101176093	13.139	291.72978	1.99585	22.5	(2.9)	sap
101177353	14.854	291.73172	0.48137	33.8	3.8	man
101178248	12.382	291.73310	0.10137	21.7	2.6	sap
101179555	13.581	291.73508	-0.39958	33.7	4.2	man
101181202	14.437	291.73759	-0.01584	22.9	(3.0)	man
101181479	13.118	291.73807	0.04918	34.6	3.8	sap
101184157	13.862	291.74223	0.16147	26.9	(2.9)	sap
101187485	14.342	291.74754	0.59697	27.8	3.6	sap
101187777	13.860	291.74796	1.62582	31.4	(4.0)	sap
101188939	14.715	291.74977	1.67190	30.7	(3.3)	sap
101189140	14.964	291.75011	0.35472	28.1	(3.0)	man
101189811	14.071	291.75112	-0.42451	34.1	(4.3)	man
101191330	14.452	291.75344	0.72945	30.2	(3.4)	man

Table 1. continued.

CoRoT-ID	m_v	ra (degrees)	dec (degrees)	ν_{max} (μ Hz)	$\Delta\nu$ (μ Hz)	selection
101192102	13.978	291.75470	1.11048	30.6	(3.5)	sap
101192695	13.409	291.75556	2.05615	33.7	(4.2)	sap
101193334	14.642	291.75656	0.58980	53.1	5.7	man
101194293	14.732	291.75803	1.83780	26.8	3.5	man
101194709	14.719	291.75870	2.06235	23.2	(2.7)	man
101195199	13.029	291.75951	1.97382	28.6		sap
101195523	13.558	291.76002	1.83068	37.1	4.3	sap
101196210	14.672	291.76113	0.66281	29.8		man
101197556	13.351	291.76320	-0.54024	34.1	3.8	sap
101197732	13.661	291.76348	-0.51246	15.9	(2.1)	man
101199197	14.202	291.76571	0.60905	28.8		man
101200044	14.406	291.76701	1.43179	28.6	(3.4)	man
101201987	14.311	291.77004	-0.11180	15.1	(2.2)	man
101202518	14.944	291.77087	1.89952	28.6	(3.3)	man
101203233	14.285	291.77201	1.75953	58.3	(5.5)	sap
101204408	13.579	291.77378	0.53474	17.5	2.3	man
101207562	12.718	291.77866	1.28381	32.7	(4.1)	sap
101207636	13.951	291.77877	-0.09446	49.9	5.4	man
101208801	14.203	291.78065	1.14579	14.1	(2.3)	man
101212236	13.905	291.78602	1.86924	34.9	4.0	sap
101214403	13.788	291.78940	1.10562	21.0	(2.8)	man
101214882	14.832	291.79015	0.21392	36.4	(4.1)	man
101216430	14.988	291.79263	1.37272	25.0		man
101217274	13.932	291.79390	0.59959	88.8	(8.1)	man
101218811	13.462	291.79639	1.86938	34.0	3.9	sap
101219553	13.894	291.79762	0.44281	102.3	(9.1)	man
101222229	14.746	291.80178	-0.45017	34.0	(4.0)	man
101222796	13.065	291.80264	0.42683	12.9	1.5	man
101223476	14.946	291.80364	-0.19615	16.8	2.2	man
101226184	15.033	291.80793	1.31134	27.1	(3.4)	man
101229068	13.501	291.81262	-0.54603	51.4	5.3	sap
101229072	13.428	291.81263	1.19002	74.3	6.9	man
101229714	13.822	291.81360	0.15832	27.8	3.5	sap
101231842	12.473	291.81682	1.97938	30.8	3.5	sap
101232297	12.476	291.81754	-0.26094	37.7		sap
101232883	14.527	291.81846	1.45619	28.7		man
101233006	13.837	291.81862	-0.07616	23.8	(3.0)	man
101234832	13.251	291.82150	-0.46851	30.7	3.8	sap
101235724	13.378	291.82294	1.85331	36.3	4.2	sap
101237841	12.706	291.82626	-0.31012	13.7	1.5	sap
101238328	12.627	291.82705	0.15114	37.2	(3.8)	sap
101239347	14.198	291.82864	1.19585	27.6	3.5	man
101239581	14.277	291.82904	0.75192	26.3		man
101241291	14.592	291.83182	1.88469	25.0		man
101242228	13.097	291.83330	0.75421	28.8	(3.7)	sap
101243695	13.623	291.83566	1.25006	13.7	1.8	man
101245682	14.479	291.83889	1.95751	22.3	(2.4)	man
101245919	13.657	291.83930	0.70098	33.7	4.1	sap
101246426	14.245	291.84015	0.49469	27.0	3.4	sap
101246686	14.351	291.84056	-0.53971	28.7		man
101246687	14.865	291.84056	1.53945	30.0	(3.1)	man
101247114	14.167	291.84118	-0.08511	32.0	4.0	man
101248026	13.281	291.84260	-0.51509	50.8	(5.0)	sap
101248294	13.559	291.84304	1.89417	30.3	(3.8)	sap
101251252	13.721	291.84776	1.32805	64.6	6.5	sap
101252836	13.833	291.85026	0.99847	22.7	(3.1)	sap
101253078	14.121	291.85064	-0.51641	15.4	2.0	man
101253113	14.526	291.85068	-0.41695	27.1		man
101254020	13.576	291.85211	-0.46991	43.0	4.7	sap
101258619	12.757	291.85924	-0.00033	37.7	4.4	sap
101260646	13.588	291.86251	1.36033	87.7	8.1	man

Table 1. continued.

CoRoT-ID	m_v	ra (degrees)	dec (degrees)	ν_{max} (μ Hz)	$\Delta\nu$ (μ Hz)	selection
101262546	14.217	291.86558	0.73952	21.2	(2.8)	man
101262678	13.761	291.86579	-0.07394	34.4	(4.1)	sap
101262795	14.156	291.86599	1.00213	30.4	3.8	sap
101264567	14.947	291.86885	0.40868	30.1	4.0	man
101265048	12.997	291.86964	0.27481	33.1	4.1	sap
101265141	13.017	291.86979	0.29741	24.6	3.0	sap
101267794	15.175	291.87398	0.51590	23.6		man
101270424	13.143	291.87795	1.68065	33.7	4.1	sap
101270438	12.889	291.87798	0.03079	15.1	2.0	sap
101271394	13.488	291.87939	-0.06955	24.8	(3.1)	sap
101272355	15.081	291.88072	0.82882	25.1	3.1	man
101273102	12.581	291.88183	-0.47210	26.9	(3.3)	sap
101273107	14.206	291.88184	-0.31577	9.5	(1.0)	man
101275308	12.828	291.88504	1.40820	25.4	(3.3)	sap
101275997	13.529	291.88602	0.73522	20.1	(2.5)	sap
101278229	14.591	291.88925	0.56474	25.9	3.1	man
101279871	15.366	291.89169	1.17678	16.7	2.4	man
101279963	13.331	291.89183	-0.52641	52.1	(5.2)	sap
101281195	14.370	291.89367	0.39727	15.9	2.2	man
101281824	12.800	291.89463	1.32962	27.4	3.3	sap
101281996	13.705	291.89490	-0.03212	28.7	(3.2)	sap
101286739	13.240	291.90217	0.95468	30.5	(3.8)	sap
101287608	15.664	291.90341	0.20226	13.0	2.0	man
101289231	13.782	291.90589	1.58396	28.9	(3.8)	man
101289267	13.401	291.90596	1.71057	35.6	(4.2)	sap
101289675	13.013	291.90657	0.94287	27.6		sap
101290029	13.174	291.90710	1.52946	27.6	(3.6)	sap
101290292	13.704	291.90751	0.59387	19.9	2.5	man
101290847	13.204	291.90835	1.21587	60.1	5.8	sap
101291471	12.502	291.90929	1.03558	36.8	(4.3)	sap
101292808	14.639	291.91129	1.01110	31.0	(3.9)	man
101295016	12.842	291.91455	-0.02784	24.6	(3.0)	sap
101296374	14.818	291.91662	0.46522	21.7	(2.9)	man
101299401	13.194	291.92123	0.13697	26.7	(3.7)	sap
101300965	14.804	291.92364	0.05322	25.3	(3.4)	man
101301023	14.178	291.92374	-0.02262	34.1		man
101303810	15.400	291.92815	1.54780	26.2		man
101303931	14.845	291.92835	1.25212	28.8	3.9	man
101304467	14.966	291.92923	0.72475	32.6	(4.1)	man
101304738	14.515	291.92964	-0.12426	28.2		man
101305294	13.725	291.93049	1.76328	36.3	(4.1)	sap
101305676	12.306	291.93106	0.21048	30.0	3.9	sap
101308337	14.296	291.93533	-0.31556	26.8	(2.8)	sap
101309464	13.939	291.93720	0.17960	33.6	(4.3)	man
101312180	13.927	291.94150	0.31710	34.6	(4.1)	man
101312308	14.214	291.94169	-0.41716	17.1	(2.1)	man
101312396	13.708	291.94182	1.41227	34.6	4.2	sap
101312732	14.625	291.94236	0.18405	18.8	2.7	man
101314527	13.392	291.94555	-0.07234	59.2		man
101315033	14.529	291.94652	1.42221	25.2	(2.8)	man
101315056	13.908	291.94658	1.27239	26.7	3.1	sap
101316136	13.301	291.94885	0.06353	28.2	(2.9)	man
101316534	13.995	291.94970	1.76776	20.4	(2.5)	man
101316698	13.418	291.95001	1.26016	32.6	4.1	sap
101319931	14.705	291.95660	0.72060	30.1	(4.0)	man
101319975	13.411	291.95672	-0.42760	30.6		sap
101320312	13.108	291.95742	1.32746	27.6	3.8	sap
101320378	13.251	291.95756	0.32240	32.9	4.1	man
101320586	13.354	291.95804	1.35960	58.3	(6.2)	sap
101321936	14.252	291.96075	1.55702	28.5	(3.7)	man
101322703	12.815	291.96227	1.05358	45.2	4.6	sap

Table 1. continued.

CoRoT-ID	m_v	ra (degrees)	dec (degrees)	ν_{max} (μ Hz)	$\Delta\nu$ (μ Hz)	selection
101322820	13.976	291.96251	0.18840	31.2	(3.3)	sap
101324332	12.771	291.96545	0.26763	52.4	(5.3)	sap
101325039	14.986	291.96688	0.69927	17.1	(1.8)	man
101326028	14.331	291.96885	-0.37445	33.6	(4.0)	man
101326609	13.931	291.97006	-0.36128	23.6	(3.0)	sap
101326879	13.241	291.97062	0.60193	34.4	4.1	sap
101331140	14.691	291.97935	-0.21837	56.3	(5.9)	man
101332107	12.884	291.98126	0.50582	29.5		sap
101332727	15.728	291.98246	0.64177	30.3	3.7	man
101332883	13.420	291.98278	0.72298	41.0	4.5	sap
101335441	13.481	291.98791	-0.24230	55.2	5.9	sap
101335883	14.860	291.98879	1.12626	52.0	5.1	man
101336091	12.891	291.98920	-0.19441	35.3	(4.0)	sap
101336195	13.772	291.98940	0.01402	17.6	(2.3)	man
101339201	12.448	291.99554	1.39588	44.7	4.8	sap
101339420	13.281	291.99600	-0.44769	17.1	(2.3)	man
101340626	14.056	291.99855	0.75001	23.3	2.7	man
101343519	13.655	292.00464	1.09325	30.2		sap
101347468	13.481	292.01276	-0.25095	34.0	4.3	sap
101347642	12.721	292.01310	-0.35930	31.9	3.9	sap
101347760	13.031	292.01333	0.26870	27.1	(2.9)	sap
101349437	14.117	292.01666	1.61570	21.1	3.1	man
101352174	13.196	292.02216	-0.35694	31.1	3.9	sap
101353737	12.952	292.02529	1.02912	62.3	5.8	sap
101355793	14.674	292.02954	1.33194	26.0		man
101356220	13.861	292.03043	0.69364	23.5	(2.4)	man
101356616	14.121	292.03123	0.88493	26.4	(3.5)	man
101358149	14.352	292.03431	-0.07450	32.1	(3.8)	man
101362519	14.420	292.04321	0.61949	28.4	(3.8)	man
101362522	13.898	292.04322	0.83149	49.9	5.5	sap
101363981	14.580	292.04619	1.04002	17.6	1.8	man
101364068	13.521	292.04636	-0.33343	21.8	(2.8)	sap
101365233	14.592	292.04878	0.90574	15.6	2.4	man
101365347	15.231	292.04900	-0.20824	20.8	(2.9)	man
101366598	13.849	292.05161	1.48692	32.3	(3.9)	sap
101368062	14.511	292.05493	-0.33227	27.3	(2.8)	man
101368866	14.851	292.05684	0.25502	29.5	(3.4)	man
101368951	12.407	292.05703	0.45265	35.4		sap
101369568	14.521	292.05857	-0.38716	31.0		man
101369666	14.290	292.05885	0.58117	15.6	(2.4)	man
101371690	13.095	292.06471	0.42102	33.0	(3.5)	sap
101372310	13.456	292.06654	0.76842	44.0	4.6	sap
101372675	15.062	292.06745	0.09699	33.7	4.0	man
101373582	15.071	292.06940	0.38306	27.7	3.0	man
101376555	13.378	292.07480	0.82183	32.4	4.0	sap
101378314	14.105	292.07787	1.18485	17.8	(2.0)	man
101378387	13.551	292.07798	-0.37571	33.3	(4.0)	sap
101378749	13.745	292.07864	-0.41542	22.8	2.9	sap
101378905	13.013	292.07888	1.37995	26.8	2.9	sap
101378942	12.755	292.07893	1.09052	13.9	2.0	sap
101378942	12.755	292.07893	1.09052	13.9	2.0	man
101380751	13.271	292.08202	0.02348	42.1		sap
101381379	14.900	292.08309	1.04161	22.8	3.0	man
101385073	14.085	292.08946	0.64575	38.4	4.3	sap
101385320	14.728	292.08990	0.60888	19.6	2.7	man
101385870	14.495	292.09083	0.87539	30.2	(3.0)	man
101386354	12.706	292.09167	-0.36107	20.5		sap
101387138	14.558	292.09297	1.46212	27.3	(3.6)	man
101391721	14.097	292.10092	-0.00401	25.6		sap
101392868	13.866	292.10289	0.14535	23.5	2.6	sap
101393792	14.571	292.10450	0.43682	24.7	(2.5)	man

Table 1. continued.

CoRoT-ID	m_v	ra (degrees)	dec (degrees)	ν_{max} (μ Hz)	$\Delta\nu$ (μ Hz)	selection
101398481	12.452	292.11263	0.89308	35.6	(3.7)	sap
101402017	12.927	292.11881	0.00253	49.6	(5.3)	sap
101402532	13.563	292.11970	1.35305	27.7		man
101403032	15.216	292.12058	0.12008	31.5	3.8	man
101403073	14.537	292.12066	0.89040	33.9	(4.1)	man
101404415	15.371	292.12298	-0.28002	14.2	2.1	man
101405957	13.794	292.12572	0.52333	38.5	4.6	man
101406318	12.601	292.12635	-0.05400	35.7	4.0	sap
101407436	13.896	292.12823	-0.35164	25.6	3.3	sap
101408422	13.622	292.12989	-0.04569	56.6	5.7	man
101409181	13.051	292.13122	-0.14648	68.0	6.6	sap
101411168	12.447	292.13457	0.14694	34.3	(4.1)	sap
101411659	12.511	292.13531	-0.33381	61.8	(5.6)	man
101412091	14.064	292.13609	0.93705	28.5		man
101413056	14.902	292.13770	-0.01829	12.1	1.6	man
101415641	13.852	292.14207	0.70118	29.9	3.8	sap
101417670	13.811	292.14555	0.70250	13.2	1.9	man
101418465	13.171	292.14694	-0.26049	59.3	5.9	sap
101419045	14.261	292.14794	0.42470	29.1	(3.7)	man
101422280	15.116	292.15342	-0.21793	67.2	(6.7)	man
101423629	13.392	292.15564	0.14282	30.4	(3.9)	sap
101424698	14.149	292.15755	0.52573	74.4	7.4	man
101425849	14.878	292.15957	0.32844	22.4	3.0	man
101426117	14.581	292.16008	0.11045	17.2	2.7	man
101426170	13.236	292.16017	0.34969	35.1	4.0	sap
101427312	14.315	292.16209	-0.10034	30.3	3.6	man
101427327	13.900	292.16211	1.30295	16.9	2.4	man
101427969	14.876	292.16329	0.39829	63.4	6.2	man
101430573	12.578	292.16786	-0.17203	22.0	(2.6)	sap
101432067	13.667	292.17052	0.19722	26.0	(3.2)	man
101433432	13.521	292.17275	0.04984	31.2	(3.7)	sap
101433941	13.710	292.17354	1.07809	29.2		man
101439884	13.781	292.18389	-0.31834	33.6	3.9	sap
101440659	13.521	292.18521	0.92757	8.9	1.4	man
101441726	14.722	292.18700	-0.06462	27.5		man
101442365	12.503	292.18808	0.63520	38.9	4.3	sap
101442374	14.161	292.18810	-0.17184	25.5	2.7	man
101444217	14.541	292.19130	0.47664	51.6		man
101446191	13.718	292.19465	0.61590	31.1	4.0	sap
101446216	14.181	292.19470	0.71501	24.7	(3.4)	man
101447328	14.641	292.19653	0.54924	25.7		man
101448392	14.601	292.19826	-0.36813	31.0	3.9	man
101448417	13.947	292.19830	0.40492	53.6	5.7	sap
101451115	13.395	292.20289	0.08869	25.6	(3.4)	man
101451373	12.347	292.20331	0.49616	32.4	(4.1)	sap
101451533	13.837	292.20357	0.46766	40.2		sap
101454067	13.631	292.20777	0.37357	32.3	(4.1)	sap
101458937	13.222	292.21625	0.17364	14.5	2.1	man
101460486	13.503	292.21880	0.81992	34.7	4.0	sap
101460775	14.761	292.21929	0.51695	42.3	4.6	man
101460879	14.585	292.21943	0.83847	65.4	6.5	man
101465171	13.802	292.22675	0.09967	21.5		man
101467619	14.261	292.23090	0.04907	31.7	4.0	man
101469820	14.360	292.23460	1.11314	16.5	2.1	man
101473616	13.945	292.24089	0.52904	18.7	2.3	man
101474112	13.892	292.24176	0.10558	62.4	6.5	man
101474730	14.151	292.24286	0.24934	22.6	2.6	man
101476440	12.951	292.24578	0.46899	12.3	1.7	sap
101476920	14.838	292.24660	0.61513	15.3	2.1	man
101477247	14.987	292.24719	0.71147	14.9	(1.6)	man
101478540	12.721	292.24933	-0.32656	22.7	2.7	sap

Table 1. continued.

CoRoT-ID	m_v	ra (degrees)	dec (degrees)	ν_{max} (μ Hz)	$\Delta\nu$ (μ Hz)	selection
101479332	13.851	292.25070	0.54807	32.7	4.1	sap
101479386	13.007	292.25080	0.46425	26.7	(3.4)	sap
101479567	12.611	292.25106	0.74391	25.1	(3.1)	man
101479905	14.088	292.25164	0.97540	26.3		man
101480480	14.991	292.25263	0.28173	16.3	2.2	man
101480733	14.071	292.25310	0.59013	44.7	5.0	man
101481433	13.846	292.25433	-0.18910	32.7	(3.9)	sap
101483826	12.707	292.25852	0.41784	26.9	(3.5)	sap
101490360	12.744	292.26966	0.91643	59.7	6.0	sap
101495773	13.786	292.27900	-0.07316	38.1	4.1	sap
101496643	13.315	292.28042	0.02775	25.6	3.3	sap
101499895	13.527	292.28593	0.19790	64.9	6.1	sap
101503482	13.753	292.29207	0.59820	22.8	3.0	sap
101509360	13.056	292.30230	-0.18344	55.5	5.7	sap
101511309	14.298	292.30568	0.66261	35.4	4.1	sap
101513155	12.978	292.30891	0.97732	32.5	4.2	sap
101513442	14.316	292.30940	0.16418	30.0		sap
101520144	12.801	292.32107	0.83685	13.3	(1.9)	man
101521149	14.755	292.32290	0.60598	32.0	(3.8)	man
101522290	12.122	292.32492	-0.03924	24.9		sap
101523962	12.267	292.32779	0.92039	27.0	(2.9)	sap
101525862	14.023	292.33117	0.81941	19.7		man
101528536	15.171	292.33599	0.51945	24.6		man
101529924	14.206	292.33835	-0.29341	24.6		man
101536163	14.471	292.34943	0.01349	21.4	2.8	man
101536782	14.781	292.35050	0.15965	22.3	2.6	man
101538074	13.358	292.35279	-0.16142	30.5	(3.8)	sap
101538346	14.181	292.35333	0.28585	28.1	3.3	man
101538547	14.217	292.35370	-0.01102	10.6	1.7	man
101538672	13.831	292.35390	-0.18196	35.6	3.7	sap
101539993	14.751	292.35622	-0.22621	23.4		man
101542075	14.827	292.35992	0.49076	12.8	1.9	man
101544311	13.749	292.36378	0.56235	33.2	4.0	sap
101546354	13.351	292.36739	0.74518	29.2	(3.6)	sap
101546964	12.901	292.36851	0.61542	24.7	2.8	sap
101550759	13.134	292.37523	0.07752	23.1	(3.2)	sap
101554715	14.398	292.38161	0.54842	29.4		man
101557699	15.160	292.38631	0.70108	33.0	(4.1)	man
101557896	13.091	292.38659	-0.21769	35.2	(3.7)	sap
101558507	13.805	292.38756	0.74707	34.0	4.2	sap
101561050	12.468	292.39166	0.25915	32.8	4.0	sap
101561081	14.313	292.39170	0.09368	32.4	(3.8)	man
101562508	13.141	292.39400	0.14149	26.9	3.7	sap
101563951	13.816	292.39623	0.64370	28.5	3.6	sap
101565025	13.626	292.39802	-0.29366	25.8		sap
101566235	14.663	292.39992	0.72789	30.3	(4.0)	man
101568144	14.259	292.40298	0.75055	21.2	3.2	man
101569001	14.191	292.40440	0.60189	38.3	(4.0)	sap
101569925	13.162	292.40580	0.51492	32.4	(3.2)	sap
101575148	13.421	292.41431	-0.17525	28.5	(3.0)	sap
101579183	13.535	292.42087	0.08014	27.8	(3.5)	sap
101579756	13.394	292.42182	-0.22418	28.4	3.7	sap
101587725	14.736	292.43463	0.43942	21.5	2.7	man
101589817	13.574	292.43818	0.12807	32.7	(3.2)	sap
101593684	14.586	292.44514	-0.01746	32.6	4.1	man
101594911	13.688	292.44738	0.64048	31.1	3.7	sap
101601779	14.161	292.46087	0.16955	14.9	2.1	man
101602667	14.651	292.46271	-0.17588	26.0	3.5	man
101602989	14.646	292.46334	0.10876	59.3	(6.2)	man
101606835	14.431	292.47106	-0.20674	27.9		man
101610551	12.301	292.47868	-0.03471	17.6	2.1	man

Table 1. continued.

CoRoT-ID	m_v	ra (degrees)	dec (degrees)	ν_{max} (μ Hz)	$\Delta\nu$ (μ Hz)	selection
101611062	14.597	292.47972	0.35666	32.5	(4.1)	man
101612565	13.132	292.48275	0.39426	22.2	2.9	sap
101614830	13.861	292.48737	0.20515	31.6	(3.5)	man
101615168	14.571	292.48798	-0.25639	22.3	3.0	man
101615645	13.242	292.48895	0.39546	41.5	4.4	sap
101616298	13.651	292.49025	-0.03199	28.3		man
101617139	14.731	292.49202	-0.22664	35.7	(4.1)	sap
101619414	13.126	292.49682	-0.10495	23.8	3.2	sap
101622423	14.531	292.50273	-0.20858	31.2	(4.0)	sap
101622447	13.513	292.50279	0.45704	50.4	5.4	sap
101623741	14.873	292.50546	0.51612	27.5	(3.5)	man
101624626	13.411	292.50721	0.00984	42.9	(4.7)	sap
101626655	13.721	292.51126	-0.16312	28.8		man
101627819	14.621	292.51362	0.17405	27.1		man
101628552	12.791	292.51520	-0.27208	33.7	(3.7)	sap
101629794	13.856	292.51781	-0.10947	26.5		man
101634748	13.561	292.52832	0.02923	31.1	3.7	man
101634822	14.966	292.52848	0.14526	24.9	(3.4)	man
101635594	13.493	292.53015	0.41928	26.7	3.2	sap
101636040	15.211	292.53111	0.00377	35.7		man
101638419	13.191	292.53611	0.02765	31.9	3.9	sap
101641463	13.933	292.54243	0.45391	28.3	3.5	man
101642089	13.681	292.54376	0.21842	29.4	3.9	sap
101645783	13.056	292.55145	-0.10843	22.7		sap
101649216	12.461	292.55934	-0.12285	19.4	(2.5)	sap
101650702	13.931	292.56421	-0.08882	12.6	1.9	sap
101650995	15.061	292.56561	-0.23266	25.0		man
101654204	13.586	292.57313	-0.24215	22.7		sap
101661981	14.084	292.58634	0.09157	25.9	2.8	man
101663605	13.471	292.58911	0.01487	26.1	(3.5)	sap
101665008	13.556	292.59157	0.31293	62.2	6.2	man
101681840	13.861	292.62024	0.08071	27.1	(3.6)	man
101686314	13.926	292.62820	0.18007	26.0		sap
101692807	13.611	292.63977	-0.19429	12.4	(1.8)	man
101701086	13.266	292.65412	0.12279	26.5		sap
101708276	13.528	292.66683	0.05302	32.7	(3.8)	sap
101737168	14.161	292.71810	-0.01920	46.2	4.8	man
101737628	14.271	292.71886	0.05476	27.1	(3.6)	man
101741393	14.184	292.72543	-0.12764	19.7	(2.7)	man
101748322	12.624	292.73779	-0.13966	52.6	5.3	sap
101753179	13.976	292.74625	-0.09557	24.7	(3.3)	man
101758645	14.386	292.75604	-0.04209	30.8	3.8	man
110567305	14.681	290.98111	1.25287	52.3	5.3	man
110569726	14.381	291.06331	1.01500	33.5		man
110635144	14.788	290.94869	0.82256	35.0		sap
110637723	12.714	291.03788	0.79087	21.4	(2.8)	man
110639075	12.747	291.11563	0.77863	36.3	4.3	sap
110649535	12.769	292.05737	1.49732	78.9	7.9	sap
110651396	13.492	292.16917	0.51249	23.5	2.7	man